Proceedings of the World Congress on Mechanical, Chemical, and Material Engineering (MCM 2015)
Barcelona, Spain – July 20-21, 2015
Paper No. 318

Sintering of Al_2O_3–Ceo_2nanopowder Prepared by Co-Precipitation Method

S.A. Hassanzadeh-Tabrizi
Advanced Materials Research Center, Materials Engineering Department, Najafabad Branch, Islamic Azad University, Najafabad, Isfahan, Iran
tabrizi1980@gmail.com

E. Taheri-Nassaj
Tarbiat Modares University, Department of Materials Science and Engineering
Tehran, Iran.
taheri@modares.ac.ir

Abstract -In the present work, Al_2O_3-CeO_2 composite nanopowders were synthesized via co-precipitation method. The sinterability of the synthesized powders was investigated. The results showed that the transformation of transition phases of alumina to α-Al_2O_3 takes place at 1200 °C. TEM images showed that the powders was composed of nanoparticles in the range of 30−70 nm. The densification of composites started at about 1200 °C. The relative density of sintered Al_2O_3-CeO_2 composites was measured to be 95% at 1600 °C. SEM results of sintered samples showed a sub-micronic/ micronic microstructure.

Keywords**:** Chemical synthesis, Nanostructures, Alumina-Ceria, Sintering.

1. Introduction

Alumina is an important ceramic in industrial applications (Schel et al., 1989 & Hassanzadeh-Tabrizi & Taheri-Nassaj, 2009), ceramic membranes and catalytic membranes (Cho et al., 1997 & Torrecillas et al., 2007). Alumina properties such as high specific surface area, surface acidity, chemical stability, and defects in their crystalline structures are the important factors in such wide range of applications (Li & Gao, 1999). Ceria is a fluorite-structured ceramic material that does not show any known crystallographic change from room temperature up to its melting point (2700 ºC) (Li et al., 2004). The mechanical properties and catalytic performance of alumina ceramics can be improved by dispersing ceria particles in alumina matrix (Hassanzadeh-Tabrizi & Taheri-Nassaj, 2011 & Heidy et al., 2015). The sintering behaviour and the microstructure of ceramics are significantly affected by the ceramic processing including the initial powder state, particle size, and sintering processes. It is known that the synthesis method has an important effect on the powder characteristics (Bowen & Carry, 2002, Li & Gao, 2001 & Pournajaf et al., 2014).

Conventional methods for synthesizing ceramic nanopowders include mechanochemical (Davoodi et al., 2015), co-precipitation (Liu et al., 2015), sol–gel (Ahmed & Abdel-Messih, 2011 & Motlagh et al., 2015), hydrothermal (Fang et al., 2015) and microemulsion synthesis (Pournajaf et al., 2014) and other related methods. Among these methods, chemical syntheses produce fine particles of high purity and high specific surface area. In addition chemical syntheses achieve intimate mixing of reactant cations on the atomic level, leading to lowering synthesis temperature. Compared with chemical methods, homogeneous precipitation method is one of the most promising techniques because of the inexpensive starting materials, a simple synthesis process and commonly available apparatus.

In the present work, Al_2O_3-CeO_2 nanocomposite powder was synthesized using the through a precipitation method. The sinterability of this nanopowder was investigated in detail.

2. Experimental Procedure

The precursor solutions for Al_2O_3–15 wt.% CeO_2nanopowder were prepared by co-precipitation method using $AlCl_3 \cdot 6H_2O$ (Merck), Al powder, $CeCl_3 \cdot 7H_2O$ (Merck), HCl (Merck) and NH_4OH (Merck). The aluminum powder was produced by M.A. University. This powder has a spherical shape with an average diameter about 37.5 μm. First $AlCl_3 \cdot 6H_2O$ and $CeCl_3 \cdot 7H_2O$ were dissolved in deionized water and HCl. Then aluminum powder was added to the solution. The precursor solution was continuously stirred at 100 °C for 4 h to completely dissolve the starting materials. The solution was added drop-wise to NH_4OH while keeping a constant pH value of 9 by adding extra-ammonia solution. The obtained precipitate was washed using distilled water to remove the impurities, and finally dried at 80 ºC for 48 h. The resultant synthesis product has been calcined at 800 °C for 30 min to remove water and volatile components. The powders were pressed into compacts, using a uniaxial press at the pressure of 300 MPa. The compacts were then sintered in a tube furnace under air atmosphere at various temperatures for 3 h with a heating rate of 6 ºC/min.

X-ray diffraction (XRD) was carried out for phase analysis of the dried precipitate and calcined powder using Philips X-pert model with CuKα radiation. The average crystallite size of the powder was estimated from the Scherrer equation. The densities of the sintered specimens were measured by the Archimedes method. The microstructures of the specimens were observed by scanning electron microscopy (SEM, XL30-Phillips) and transmission electron microscopy (TEM, CM200-FEG-Phillips).

3. Results and Discussion

The X-ray diffraction patterns of the precipitate heat treated for 3 h at various temperatures are shown in Fig. 1. As can be, the dried precipitate consists of CeO_2 with pure cubic structure and AlOOH. By increasing the heat treatment temperature to 400 °C, bohmite changes to amorphous alumina and only the ceria peaks are detected. Amorphous alumina converts to η-Al_2O_3 at 600 °C. By increasing the temperature to 1100 °C, θ-Al_2O_3 is formed. The peak intensity of these phases increases with increasing the temperature. In addition the broadening of the peaks decreases which shows growing the nanocrystallites. Transformation of transition phases of alumina to α-Al_2O_3 takes place at 1200 °C.

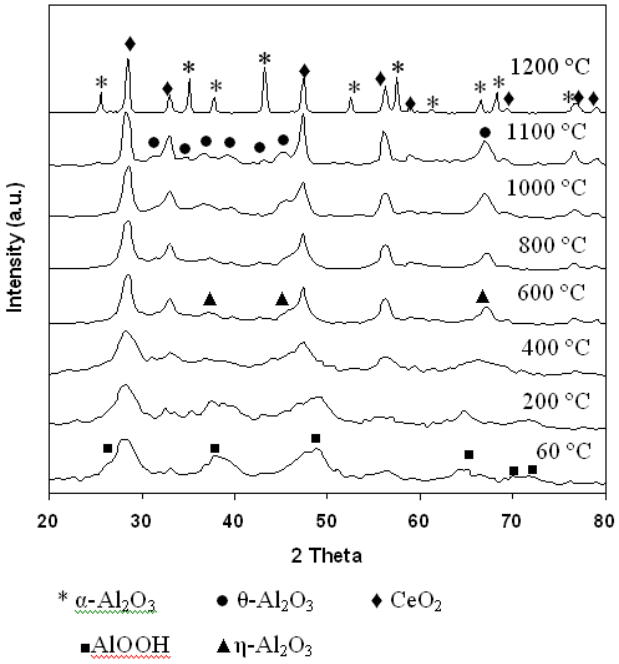

Fig. 1. XRD patterns of composite samples heat treated at various temperatures.

Fig. 2 shows the TEM image of the powders heat treated at 800 °C. As can be seen, some agglomerates exist in the powders, which are attributed to the uncontrolled coagulation during precipitation and formation of necks during calcination. The size of primary particles is in the range of 30−70 nm. In addition some agglomerates exist in the powders which are attributed to uncontrolled coagulation during precipitation. In fact the particles cling together and form larger agglomerated structures to reduce surface energy.

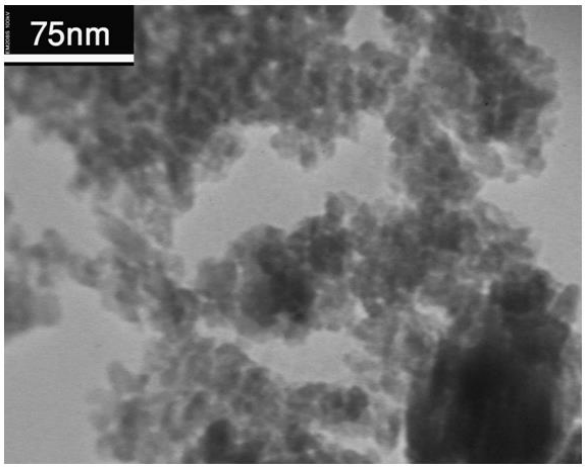

Fig. 2. TEM micrograph of Al_2O_3–15 wt.% CeO_2 powder after heat treatment at 800 °C.

Fig. 3 shows the changes of the fractional density versus the sintering temperature of Al_2O_3–15 wt.% CeO_2 composite. The density versus temperature plot exhibited a sigmoidal shape. As seen, the sintering rate below 1200 ºC was slow. The rate of densification increased drastically at 1300 C and a significant densification was obtained at about 1550 C. As a consequence, the increase of temperature from 1200 to 1550 °C increased the fractional density from 62 to 93 of theoretical density. With further increasing of the sintering temperature, a relatively slight increase was obtained in the density. One reason for limitation of density (95%) is due to dry pressing process. As it is known, by uniaxial pressing the external force can never arrive on an individual particle in the body to shift it into an optimum position between its neighbors. Therefore, this method generates large pores in green compacts. As it is known, the highest densification rate occurs for the finest pore size. Therefore, large pores in the samples undergo the pore-boundary separation and remain. It reduces the density in all sintered specimens.

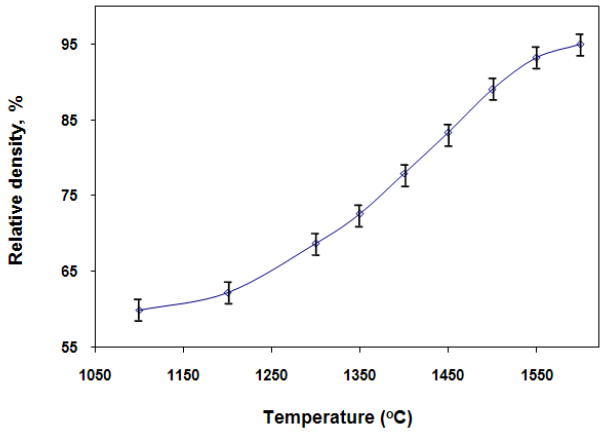

Fig. 3. Density of sintered nanocomposite powder as a function of sintering temperature.

Fig. 4 shows the changes of the grain size versus the fired temperature of Al_2O_3-CeO_2 composite. The change of grain size as a function of sintering temperature presents two distinct regions. At the first region, between 1300 and 1450 °C, the rate of grain growth was slow. In the second stage of sintering (usually between 0.65 and 0.9 theoretical density), according to the solid-state sintering mechanism, dispersed open pores could pin grain boundaries and hinder grain boundary migration, for which the grain growth was suppressed. Second region was related to temperatures higher than 1450 °C. In this region, the final grain size of the sintered samples was sharply increased. It shows a significant grain growth at the final stage of sintering. It was confirmed that the open pores (referring to the intermediate stage of sintering) collapsed to form closed pores, after which the final stage of sintering started. Such a collapse resulted in a substantial decrease in pore pinning, which triggers the accelerated grain growth.

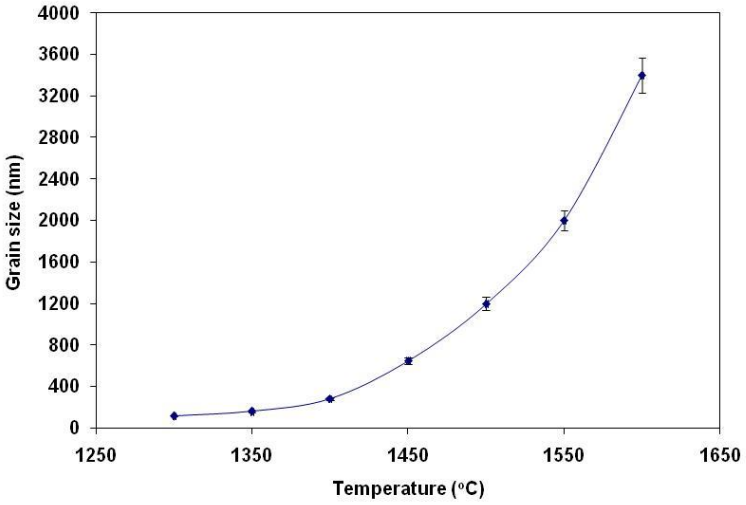

Fig. 4. Grain size of sintered nanocomposite powder as a function of sintering temperature.

The microstructure of the sample after sintering at 1600 ºC for 3 h is shown in Fig. 5. Microstructural observation showed that grain growth occurs in the samples. As can be seen, an inhomogeneous equiaxed microstructure is observed. The contrasted grey and bright areas within the images on the nanocomposites correspond to the Al_2O_3 and CeO_2 phases, respectively. Some CeO_2 particles about 500nm were located between grains. Some pores are visible in the microstructure.

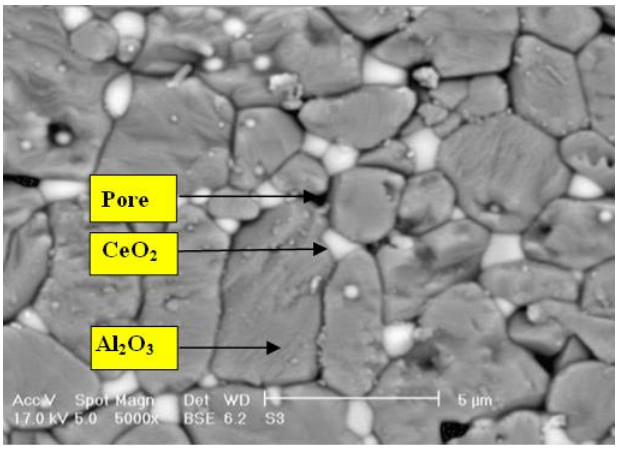

Fig. 5. Scanning electron micrograph of specimen sintered at 1600 ºC for 3 h.

4. Conclusion

In the present study an Al_2O_3-CeO_2nanopowder was synthesized via co-precipitation method. The dried precipitate consisted of CeO_2 with pure cubic structure and AlOOH. The precipitate transformed to Al_2O_3-CeO_2 at higher temperatures. Most of the particles calcined at 800 °C were in the range of 30-70 nm. The relative density of sintered composites was measured to be 95% at 1600 ºC. SEM micrograph revealed that CeO_2 particles (about 500 nm) are located between grains. SEM results of sintered samples showed a sub-micronic/ micronic microstructure.

References

Ahmed, M.A., & Abdel-Messih, M.F. (2011). Structural and Nano-Composite Features of TiO_2–Al_2O_3 Powders Prepared By Sol–Gel Method. *J. Alloys Compd.*, *509*, 2154–2159.

Bowen, P., & Carry, C. (2002). From Powders To Sintered Pieces: Forming, Transformations And Sintering Of Nanostructured Ceramic Oxides. *Powder Technol.*, *128*, 248–255.

Cho, J., Harmer, M.P., Chan, H.M., Rickman, J.M., & Thompson, A.M. (1997). Effect of Y and La on the Tensile Creep Behaviour of Aluminium Oxide. *J. Am. Ceram. Soc.*, *80*, 1013–1017.

Davoodi, D., Hassanzadeh-Tabrizi, S.A., Emami, A.H., & Salahshour, S. (2015). A Low Temperature Mechanochemical Synthesis of Nanostructured Zrc Powder by a Magnesiothermic Reaction. *Ceram. Int.*, *41*, 8397–8401

Fang, J., Huang, X., Ouyang, X., & Wang, X. (2015). Study Of The Preparation of γ-Al_2O_3 Nano-Structured Hierarchical Hollow Microspheres With A Simple Hydrothermal Synthesis Using Methylene Blue As Structure Directing Agent And Their Adsorption Enhancement For The Dye. *Chem. Eng. J.*, *270*(15), 309-319.

Hassanzadeh-Tabrizi, S.A., & Taheri-Nassaj, E. (2009). Economical Synthesis of Al_2O_3 Nanopowder Using a Precipitation Method. *Mater. Lett.*, *63*, 2274–2276.

Hassanzadeh-Tabrizi, S.A., & Taheri-Nassaj, E. (2011). The Compaction, Sintering, and Mechanical Properties of Al_2O_3–CeO_2 Composite Nanopowders. *J. Am. Ceram. Soc.*, *94*, 3488–3493.

Heidy, L., Pulgarin, C., & Albano, M.P. (2015). Three Different Alumina–Zirconia Composites: Sintering, Microstructure and Mechanical Properties. *Mater. Sci. Eng. A*, *639*, 136-144

Li, W.Q., & Gao, L. (1999). Processing, Microstructure and Mechanical Properties of 25 vol% YAG-Al_2O_3 Nanocomposites. *Nanostruct. Mater.*, *11*, 1073–1080.

Li, J., Ikegami, T., & Mori, T. (2004). Low Temperature Processing Of Dense Samarium-Doped CeO_2 Ceramics: Sintering And Grain Growth Behaviours. *Acta Mater.*, *52*, 2221–2228.

Li, W., & Gao, L. (2001). Compacting and Sintering Behavior of Nano ZrO_2 Powders. *Scripta Mater.*, *44*, 2269–2272.

Liu, J., Liu, P., Zhang, X., Pan, D., Zhang, P., & Zhang, M. (2015) Synthesis And Properties Of Single Domain Sphere-Shaped Barium Hexa-Ferrite Nano Powders Via An Ultrasonic-Assisted Co-Precipitation Route. *Ultrason. Sonochem.*, *23*, 46-52.

Mouret, G., Mozet, K., Muhr, H., Plasari, E., & Martin, M. (2009). Production of Al_2O_3–TiO_2 Catalyst Supports with Controlled Properties Using a Co-Precipitation Process. *Powder Technol.*, *190*, 84–88.

Motlagh, M.M., & Hassanzadeh-Tabrizi, S.A., (2015). Sol–Gel Synthesis of Mn2O3/Al2O3/SiO2 Hybrid Nanocomposite and Application for Removal of Organic Dye. *J Sol-Gel Sci Technol*., *73*, 9–13.

Pournajaf, R., Hassanzadeh-Tabrizi, S.A., & Ghashang, M., (2014). Effect of Surfactants on the Synthesis of Al_2O_3–Ceo_2 Nanocomposite Using a Reverse Microemulsion Method. *Ceram. Int.*, *40*, 4933–4937.

Schel, M., Diaz, L.A., & Torrecillas, R. (2002). Alumina Nanocomposites from Powder–Alkoxide Mixtures. *Acta Mater.*, *50*, 1125–1139.

Scott, M.G. (1983). *Amorphous Metallic Alloys*. Butterworths, London.

Torrecillas, R., Schehl, M., Diaz, L.A., Menendes, J.L., & Moya, J.S. (2007). Creep Behaviour of Alumina/YAG Nanocomposites Obtained By a Colloidal Processing Route. *J. Eur. Ceram. Soc.*, *27*, 143–150.

Tok, A.I.Y., Boey, F.Y.C., Dong, Z., & Sun, X.L. (2007). Hydrothermal Synthesis of CeO_2 Nano-Particles. *J. Mater. Process. Technol.*, *190*, 217–222.